STAR Protocols

CellPress
OPEN ACCESS

Protocol

Protocol for whole-cell patch-clamp recording and post hoc identification of hippocampal CA2 pyramidal neurons in adult mouse brain slices

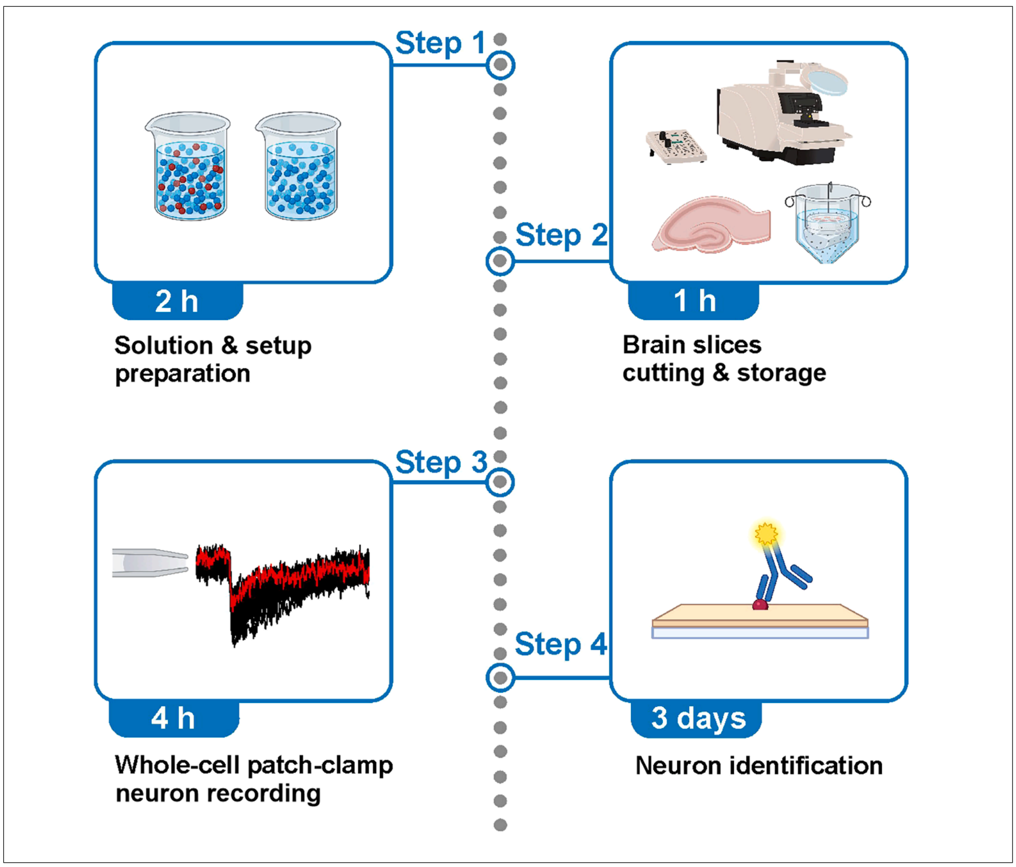

Dominique Engel, Laurent Nguyen

dominique.engel@uliege.be (D.E.)
lnguyen@uliege.be (L.N.)

Highlights

Preparation of acute dorsal hippocampal brain slices from adult mouse brain

Whole-cell patch-clamp recording from visually identified CA2 pyramidal neurons

Post hoc molecular identification and localization of recorded CA2 pyramidal neurons

We present a protocol for whole-cell recordings from hippocampal CA2 pyramidal neurons in acute adult mouse brain slices. We describe the preparation of viable dorsal hippocampal slices, the visual identification and recording of CA2 neurons, and intracellular labeling. We then detail post hoc immunohistochemical verification using CA2-specific markers. This approach enables reliable functional characterization of CA2 neurons and unambiguous confirmation of their anatomical localization.

Publisher's note: Undertaking any experimental protocol requires adherence to local institutional guidelines for laboratory safety and ethics.

Engel & Nguyen, STAR Protocols 7, 104470
June 19, 2026
https://doi.org/10.1016/j.xpro.2026.104470

STAR Protocols

CellPress
OPEN ACCESS

Protocol

Protocol for whole-cell patch-clamp recording and post hoc identification of hippocampal CA2 pyramidal neurons in adult mouse brain slices

Dominique Engel[1,3,*] and Laurent Nguyen[1,2,4,*]

[1]Laboratory of Molecular Regulation of Neurogenesis, GIGA Institute, University of Liège, 4000 Liège, Belgium

[2]WELBIO Department, WEL Research Institute, Avenue Pasteur, 6, 1300 Wavre, Belgium

[3]Technical contact

[4]Lead contact

*Correspondence: dominique.engel@uliege.be (D.E.), lnguyen@uliege.be (L.N.)
https://doi.org/10.1016/j.xpro.2026.104470

SUMMARY

We present a protocol for whole-cell recordings from hippocampal CA2 pyramidal neurons in acute adult mouse brain slices. We describe the preparation of viable dorsal hippocampal slices, the visual identification and recording of CA2 neurons, and intracellular labeling. We then detail post hoc immunohistochemical verification using CA2-specific markers. This approach enables reliable functional characterization of CA2 neurons and unambiguous confirmation of their anatomical localization.

For complete details on the use and execution of this protocol, please refer to Le Bail et al.[1]

BEFORE YOU BEGIN

This protocol describes the preparation of acute hippocampal brain slices containing the dorsal CA2 subfield and subsequent whole-cell recordings from CA2 pyramidal neurons in adult mice. Slices are prepared from the dorsal hippocampus, as this region exhibits robust expression of molecular markers that delineate the CA2 subfield and is implicated in functions such as social memory storage,[2,3] ripple generation[4] and novelty processing.[5] Sagittal slices[6–8] obtained approximately 2-4 mm from the midline[8] preserve the dorsal CA2 region and are cut perpendicular to the longitudinal axis of the hippocampus. Compared with coronal sections, sagittal slices better preserve the intrahippocampal circuitry, including the trisynaptic pathway, and hippocampal-entorhinal cortex connectivity.[9–11] In addition, many molecular markers used to delineate CA2 are enriched in the dorsal hippocampus but are weakly expressed or absent in the ventral hippocampus.[12–14] Because the borders of CA2 cannot be reliably identified in live slices using transmitted-light microscopy, recordings are performed based on anatomical criteria and are subsequently validated using post hoc histochemical or immunohistochemical labeling of CA2-specific markers.[6,7,12,15–19] This confirmation step is essential to ensure accurate assignment of recorded neurons to the CA2 subfield.

Innovation

The procedure is adapted from protocols originally developed for electrophysiological recordings in juvenile hippocampal tissue (19-26-days-old)[20,21] and incorporates specific modifications required to maintain slice viability and cellular integrity in adult (8-10 weeks-old) brain tissue. The protocol describes the preparation of sagittal slices to allow access to the dorsal hippocampus.

Institutional permissions

All animal procedures must be approved by the relevant institutional and governmental authorities before initiating experiments. The experiments described here were approved by the Ethics Committee of the University of Liège (protocols #1912, #2177 and #2455)[1] and were conducted in accordance with Belgian Ministry of Agriculture guidelines and European Community Laboratory Animal Care and Use Regulations (86/609/CEE, Journal Official des Communautés Européennes L358, 18 December 1986).

Patch-clamp recording setup

This section describes the essential components required for whole-cell patch-clamp recordings in acute hippocampal brain slices. For general information concerning the aspect and material composition of the patch-clamp setup, we refer readers to selected literature (The Axon Guide by Molecular Devices, San Jose, CA, USA; https://www.moleculardevices.com/en/assets/user-guide/dd/cns/axon-guide-to-electrophysiology-and-biophysics-laboratory-techniques, https://www.luigs-neumann.org and ref.[22–25]). In the next section, we detail the essential components for whole-cell recordings in acute hippocampal brain slices.

1. Acquire an anti-vibration table.

   Note: An anti-vibration table is required to mechanically isolate the recording chamber and micromanipulators from environmental vibrations.

   a. Connect the table either to a high-pressure nitrogen cylinder (https://mx.airliquide.com/en/packaged-gases) or to an air compressor that provides pneumatic suspension.

   Note: This setup minimizes mechanical vibrations affecting the recording chamber and manipulators.[23]

   b. Check the table suspension regularly to ensure proper vibration isolation.
2. Microscope and optics.
   a. Use an upright microscope (e.g., Zeiss Axioskop 1FS,[1,25,26] Olympus BX51 or Luigs&Neumann LNscope) to allow direct visual access to the upper surface of the slice.

   Note: Upright configurations allow direct visualization of the slice surface and precise placement of recording and stimulation pipettes. Older-generation upright microscopes remain suitable due to their mechanical stability.[26] The microscope stage may be manual or motorized.

   ⚠ CRITICAL: Inverted microscopes are not recommended, as the objective is positioned below the recording chamber.

   b. Employ for contrast either Dodt gradient contrast (DGC) optics[27] or differential interference contrast (DIC) optics.[22,23,25,28]
   c. Use high-numerical-aperture objectives and condensers (NA>0.7) to visualize the fine details of the cell membranes but also of the pipette tips.
   d. Use a 5X low magnification objective to survey the slice and a 40X or 63X water-immersion high magnification objective.

   Note: The working distance enabled by the high magnification objective (≥1 mm) must be sufficient to be able to move the pipette under the lens.

   e. Mount a digital camera on the microscope to display images on a digital screen or monitor (videomicroscopy).[22,25,28]

f. Install an infrared filter (λ_{max} = 780 nm; RG-9, Schott, Germany, or infrared filter from Luigs&-Neumann)[25,27] at the output of the light source to improve slice transparency and cellular visualization.[27,28]

⚠ CRITICAL: Optimize DIC alignment[25] and adjust Köhler illumination before recordings to achieve optimal image quality. For these adjustments, see ref.[23] and tutorial: https://www.zeiss.com/microscopy/en/resources/insights-hub/foundational-knowledge/koehler-illumination.html.

3. Patch-clamp amplifier.
   a. Use a single-electrode patch-clamp amplifier (The Axon Guide) capable of both current- and voltage-clamp recordings.[1,20,21]
   b. Connect the amplifier to a personal computer via an analog-to-digital interface for signal digitization (e.g., Digidata 1440).
4. Recording chamber.
   a. Place a submerged-type recording chamber (e.g., bath chamber 62 mm diameter Luigs&Neumann) on the microscope stage.

Note: We performed electrophysiological recordings at room temperature (20°C–25°C), but the recording chamber might be heated to near-physiological temperatures using a bath-controller (e.g., Luigs&Neumann temperature controller type TC07).

   b. Ensure the brain slice lies flat at the bottom of the chamber and remains fully submerged.
   c. Secure the slice using a custom-made platinum ring (diameter 1.5 cm) with nylon threads or a U-shaped stainless steel slice anchor from Warner Instruments (https://www.warneronline.com/slice-anchors-kits-harps.html) in order to maintain the slice in place.[22,29]
5. Bath perfusion.

Perfuse the recording chamber continuously with artificial cerebrospinal fluid (ACSF).

Note: Gravity-driven perfusion is commonly used, with the ACSF reservoir (supplemented by 95% O_2 – 5% CO_2) placed approximately 50 cm above the chamber (see Figure 1 in ref.[23]). Alternatively, use a peristaltic pump (e.g., Gilson MINIPULS 3) to recirculate the bathing medium. Recirculation of the ACSF (supplemented by 95% O_2 – 5% CO_2) allows perfusion of small or measurable volumes. If an expensive drug must be applied to block some channels for instance, prioritize recirculation of ACSF.

6. Micromanipulators.

Use highly stable, low-drift manipulators to position patch pipettes accurately such as the L&N Mini 25 (https://www.luigs-neumann.org/mini) or the Kleindiek MM3A-LS (https://www.kleindiek.com/products/life-science/mm3a-ls).

⚠ CRITICAL: Verify pipette stability under high magnification (40X) before recordings by monitoring tip drift for several minutes.

Note: To assess mechanical stability, we position a pipette with its tip centered on a cross marked with a pen at the center of the monitor and monitor for any detectable movement.

7. Slice storage chamber.

After cutting, allow slices to recover in a custom-made storage chamber consisting of a 120 mL glass beaker and a gauze support maintained by Petri dish ring.

Note: This design permits frequent replacement and thorough cleaning. An illustration and a description of this storage chamber, the "Gibb chamber", are in refs.[22,30]

⚠ CRITICAL: Keep the storage chamber extremely clean. Replace the chamber with freshly cleaned components at least monthly.

8. Recording protocols.
   Prepare acquisition protocols to generate voltage and current steps before starting experiments (e.g., Clampex, Molecular Devices).
   a. Write for current-clamp recordings a typical protocol consisting of long (1 sec) current steps of increasing amplitude (from −100 to +200 pA, increment 20 pA).
   b. Write for voltage-clamp recordings a simple protocol for holding current or a protocol consisting of brief voltage steps to monitor passive membrane properties.
9. Extracellular stimulation.

Place the isolated stimulation unit for extracellular stimulation within easy reach of the recording setup, for example next to the micromanipulator remote control panels (Figure 1 in ref.[23]).

Alternative setup components

The distinct patch-clamp setup components are listed in the key resources table. We use an Axopatch 200B amplifier for patch-clamp recordings. Other amplifiers are also suited such as the Multiclamp 700B amplifier (Molecular Devices, San Jose, CA, USA), the HEKA EPC 10 (Harvard Bioscience Inc.) or the npi SEC-10LX (npi electronic GmbH, Tamm, Germany). We use an analog to digital interface from Molecular devices, the Digidata 1440, but other interfaces can be adapted such as the CED 1401 or the CED 1401 plus (Cambridge Electronic Design).

10. Animals.
    a. Handle animals gently[20,31] and minimize stress at all stages of the procedure.

Note: Animal health and physiological state are critical determinants of slice quality and recording success.

    b. Before experiments, house animals in a quiet environment and monitor their general condition, body temperature, and behavior.

Note: The experiments described in this protocol were performed using adult male mice (8–10 weeks old) on a CD1 genetic background (Janvier Labs, Saint-Berthevin, France).[1,32]

Solution preparation (external and internal solutions)

Timing: ∼2 h

11. External recording solution.
    a. Use artificial cerebrospinal fluid (ACSF) for both slice storage and recordings.

Note: Prepare ACSF on the day of the experiment whenever possible.

    b. Prepare ACSF according to Table 1 using double-distilled water (resistivity ≥18 mΩ·cm).

Note: The target osmolarity is ∼320 mOsm (acceptable range: 314–325 mOsm) with 95% O_2 and 5% CO_2 and a final pH of 7.4.

Table 1. Standard physiological saline (aCSF)

Substance	MW molecular weight in g/mol	Final concentration	Amount g/1 L
NaCl	58.44	125 mM	7.306
$NaHCO_3$	84.01	25 mM	2.1
KCl	74.56	2.5 mM	0.187
NaH_2PO_4	137.99	1.25 mM	0.173
Glucose	198.17	25 mM	4.954
$MgCl_2$	203.3	1 mM	0.203
$CaCl_2$	147.02	2 mM	0.294

pH=7.4, osmolarity: 320 mOsm.

c. Measure osmolarity using a freezing-point osmometer (e.g., Gonotec).
d. Store at 4°C for up to 3 days.
e. For pharmacological isolation of synaptic currents, supplement ACSF as follow:
    sEPSCs: add picrotoxin (50 μM) to block $GABA_A$ receptors.
    sIPSCs: add CNQX (10 μM) and D-AP5 (20μM) to block AMPA and NMDA receptors.
    mIPCSs: add 1 μM TTX to isolate miniature synaptic currents.
    EPSP/IPSP: SR95531 (10 μM) to block $GABA_A$ receptors and CGP 55485A (1 μM) to block $GABA_B$ receptors.
f. Prepare drug-containing ACSF fresh on the day of use.

12. External cutting solution.
    a. For adult mice, use a sucrose-based cutting solution to improve neuronal viability during brain dissection and slicing.
    b. Prepare the solution on the day of the experiment whenever possible according to Table 2.

Note: Compared with standard ACSF, this solution contains reduced Na^+ and Ca^{2+} concentrations, increased Mg^{2+}, and added sucrose.[20,26,33–35] The rationale to add sucrose and reduce NaCl in the ACSF is to reduce Na^+ influx and therefore depolarization during tissue dissection and diminish cell swelling due to chloride ions and water entry[36,37] and to favor the preservation of GABA-mediated synaptic transmission.[38]

    c. Prepare the solution using two separate 2 L glass beakers.
        i. Dissolve $NaHCO_3$ separately from the remaining salts to prevent precipitation. Chemicals must be of high purity.[26]
        ii. Oxygenate continuously the solution with 95% O_2 – 5% CO_2 gas mixture using a gas diffuser such as microfilter candles (Robu, https://www.robuglas.com/en/laboratory-equipment-robu/filter-candles-with-tube.html) to maintain pH at 7.4.

Table 2. Sucrose-based external solution for the preparation of brain slices

Substance	MW molecular weight in g/mol	Final concentration	Amount g/1 L
NaCl	58.44	87 mM	5.084
$NaHCO_3$	84.01	25 mM	2.1
KCl	74.56	2.5 mM	0.187
NaH_2PO_4	137.99	1.25 mM	0.173
Glucose	198.17	10 mM	1.981
Sucrose	342.30	75 mM	25.672
$MgCl_2$	203.3	7 mM	1.423
$CaCl_2$	147.02	0.5 mM	0.07351

pH=7.4, osmolarity: 326 mOsm.

Table 3. Pipette solution for inhibitory synaptic currents

Substance	MW molecular weight in g/mol	Final concentration	Amount g/100 mL
KCl	74.56	110 mM	0.8202
K-gluconate	234.2	30 mM	0.7026
EGTA	380.4	10 mM	0.3804
$MgCl_2$	203.3	2 mM	0.0406
Na_2-ATP	551.1	2 mM	0.1103
Hepes	238.31	10 mM	0.2383
Biocytin	2 mg/mL	–	0.2

pH=7.2 adjusted with KOH, osmolarity: 310 mOsm. A low osmolarity can be adjusted with sucrose.

Note: We use this sucrose-based solution to dissect the brain and cut slices but not for the storage of the slices.

iii. Use double distilled water (resistivity ≥18 mΩ·cm).

Note: The target osmolarity is ~326 mOsm (acceptable range: 325–330 mOsm). If the prescribed osmolarity is too low, one or several chemicals are probably missing in the solution.

iv. Store the cutting solution at 4°C for no longer than 3 days.

13. Internal (pipette) solutions.
    a. Prepare internal solutions according to the experimental objective. Compositions are listed in Tables 3, 4, 5, and 6.

Note: For all internal solutions, use double-distilled water (resistivity ≥18 mΩ·cm).

b. Use a KCl-based internal solution containing KCl and K-gluconate to record miniature inhibitory postsynaptic currents (mIPSCs) the composition of which is presented in the Table 3.

Note: Alternatively, substitute K^+ with Cs^+ to block K^+ currents[22] and use a CsCl-based pipette solution. The presence of Cs^+ improves steady-state voltage control in distal dendrites[39] and the resolution of synaptic events but depolarizes the recorded neuron. In addition, CsCl-based internal solution might compromise morphological analysis following biocytin labelling.[26]

c. Use a K^+-based solutions to examine intrinsic firing properties in current-clamp, at the beginning of the recording and/or at the end.

Table 4. Pipette solution for excitatory synaptic currents

Substance	MW molecular weight in g/mol	Final concentration	Amount g/100 mL
K-gluconate	234.2	120 mM	2.8104
KCl	74.56	20 mM	0.1491
$MgCl_2$	203.3	2 mM	0.0406
Na_2-ATP	551.1	4 mM	0.2204
Na_2-GTP	523.18	0.5 mM	0.026
Na_2-Phosphocreatine	255.1	5 mM	0.1275
EGTA	380.4	0.1 mM	0.0038
Hepes	238.31	10 mM	0.2383
Biocytin	1 mg/mL	–	0.1

Ph=7.2 adjusted with KOH, osmolarity: 310 mOsm.

Table 5. Pipette solution for EPSP-IPSP

Substance	MW molecular weight in g/mol	Final concentration	Amount g/100 mL
K-gluconate	234.2	140 mM	3.278
$MgCl_2$	203.3	1 mM	0.0203
Na_2-ATP	551.1	2 mM	0.1102
Na_2-GTP	523.18	0.3 mM	0.016
Na_2-Phosphocreatine	255.1	5 mM	0.1275
EGTA	380.4	1 mM	0.038
Hepes	238.31	10 mM	0.2383
Biocytin	1 mg/mL	–	0.1

pH=7.2 adjusted with KOH, osmolarity: 301 mOsm.

Note: The high intracellular Cl^- concentration sets the chloride reversal potential near 0 mV, increasing the driving force for inhibitory currents at a holding potential of V_h=−70 mV.

d. Use a K-gluconate-based pipette solution (Table 4) to record excitatory synaptic currents (sEPSCs).
e. Use a K-gluconate based pipette solution (Table 5) to detect EPSPs and IPSPs with large amplitude.

Note: A fluorescent tracer (e.g., 1–25 μM Alexa Fluor 594) may be added to these pipette solutions to visualize the cell during live recording.

f. Add biocytin (1 or 2 mg/mL)[20] to all internal solutions for post hoc morphological identification.

Note: Biocytin reacts with avidin coupled to a fluorochrome to allow visualization of the recorded cell.

g. Adjust pH to 7.2 using KOH for all K^+-based internal solutions or CsOH for Cs^+-based solutions.

Note: Target osmolarity is ∼310 mOsm and should be ∼10 mOsm lower than osmolarity of ACSF in order to avoid cell swelling.

h. Use the pipette solution described in Table 6 for extracellular electrical stimulation.[40]
i. From a total volume of 100 mL, aliquot 1.6 mL of solution in 2 mL Eppendorf tubes for all pipette solutions.

Note: Low osmolarity values are adjusted by adding small amounts of sucrose to the solution.

Table 6. Hepes-buffered Na^+-rich for stimulation electrode

Substance	MW molecular weight in g/mol	Final concentration	Amount g/100 mL
NaCl	58.44	135 mM	0.789
KCl	74.56	5.4 mM	0.04
Hepes	238.31	5 mM	0.120
$CaCl_2$	147.02	1.8 mM	0.026
$MgCl_2$	203.3	1 mM	0.021

pH=7.2, adjusted using NaOH.

j. Store these aliquots at −20°C for <6 months.
k. On the day of the experiment, thaw a single 1.6 mL aliquot, which is generally sufficient for one day of recordings.
l. Check systematically the osmolarity of the pipette solution before starting recordings.

Note: The osmolarity of the solution from a thawed aliquot must match the initial value; if not, discard it and thaw a new aliquot.

m. Filter the pipette solution through a 0.22 μm syringe filter before use.
n. Keep the syringe containing the pipette solution on ice.

⚠ CRITICAL: The pipette solution containing ATP, GTP, and phosphocreatine should be stored on ice to prevent degradation of these compounds.

o. Wrap the syringe using aluminum foil to protect the pipette solution from light.

Note: Pipette solution containing a fluorochrome (e.g., Alexa 564) must be protected from light to avoid photobleaching.

Preparation of glass pipettes

Timing: 30 min

This step describes how to fabricate patch pipettes from glass capillaries using a micropipette puller.

14. Fabricate patch-clamp pipettes.
    a. Use clean borosilicate glass capillaries (e.g., Hilgenberg GmbH, Malsfeld, Germany, https://www.hilgenberg-gmbh.de, outer diameter 2.0 mm, wall thickness 0.5 mm) supplied pre-washed by the manufacturer.

    Note: Thick-walled borosilicate glass cylinders are also available by World Precision Instruments (Sarasota, FL 34240, USA) or Harvard Apparatus (Holliston, MA 01746, USA).

    b. Pull patch pipettes using a programmable micropipette puller (e.g., Sutter P-97 Flaming/Brown type micropipette puller (Figure 1A) or P-1000 or DMZ Universal Electrode Puller (https://www.zeitz-puller.com)).
    c. Adjust heating parameters to control tip geometry and taper length.

    Note: The target taper length is 3–5 mm, using borosilicate glass (2 mm outer diameter and 1 mm inner diameter) and FT330B filament mounted in a Sutter P-97 pipette puller. The taper length should be sufficient to allow access to neurons when using high-magnification objectives with short working distances. Detailed guidance for optimizing puller settings is available in the helpful "pipette cookbook": https://www.sutter.com/micropipette/cookbook and in ref.[22]

    d. Pull pipettes with a resistance of 3–4 MΩ for standard whole-cell recordings,
    e. Inspect the tip of each freshly pulled pipette (Figure 1B) under a binocular loupe (35X) mounted on a microforge (Narishige, Tokyo, Japan).
    f. Ensure the pipette tip is clean and smooth.
    g. Fire-polish the tip using the microforge to improve seal formation with the cell membrane.

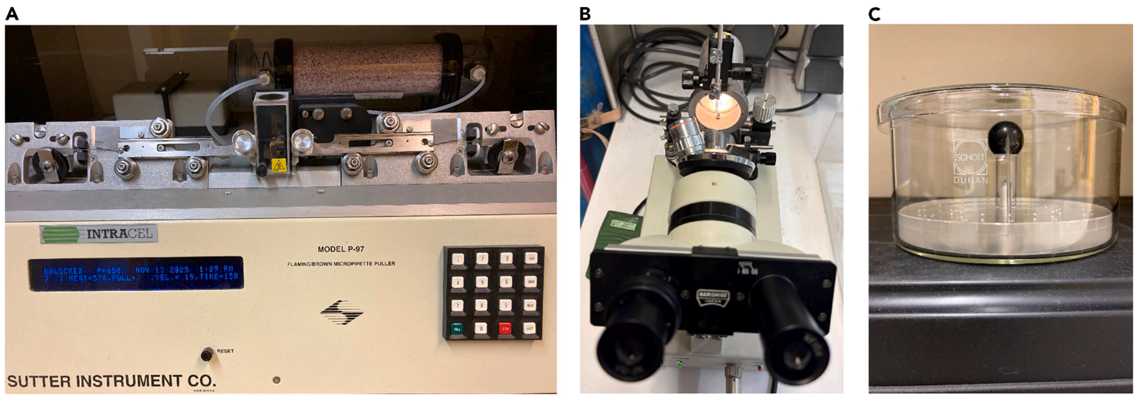

Figure 1. Preparation of recording pipettes
(A) Glass tubing installed on puller bars to produce patch pipettes.
(B) Microforge to inspect the morphology of pipette tip using a 35X objective.
(C) Glass container for the storage of freshly fabricated pipettes. A pipette with its tip to the top is in the center of the container.

h. Store the freshly fabricated pipettes vertically (tip upward) in a closed glass container with a glass lid on a custom-made support with holes to prevent dust contamination at the pipette tip (Figure 1C).
i. Fabricate pipettes from double-barreled theta (θ) glass[41] for focal extracellular stimulation.

Note: The resistance of the stimulating electrode is 4–10 MΩ.

j. Prepare and store 10–12 pipettes in a closed container before starting recordings.

Note: Use freshly pulled pipettes within 8 h of fabrication.

15. Turn on equipment.
    a. Switch on all the devices (patch-clamp amplifier, interface, manipulators, camera, light source, and computer) from the patch-clamp setup.
    b. Switch on the software (e.g., clampEx) for patch-clamp recording.

KEY RESOURCES TABLE

REAGENT or RESOURCE	SOURCE	IDENTIFIER
Antibodies		
Mouse anti-RGS14 (dilution: 1/500)	Neuromab	Cat#75-170, N133/21; RRID: AB_2877352
Rabbit anti-PCP4 (dilution: 1/500)	Sigma-Aldrich	Cat#HPA005792, RRID:AB_1855086
Biotin-conjugated Wisteria floribunda agglutinin (WFA) lectin	Sigma-Aldrich	Cat#L1516
Fluoromount aqueous medium	Sigma-Aldrich	Cat#F4680
Triton X-100	Sigma-Aldrich	Cat#T8787
Normal Donkey Serum (NDS)	Jackson ImmunoResearch	RRID: AB_2337258
Secondary antibody	Thermo Fisher Scientific	https://www.thermofisher.com/be/en/home/life-science/antibodies/secondary-antibodies/fluorescent-secondary-antibodies/alexa-fluor-secondary-antibodies.html
Chemicals, peptides, and recombinant proteins		
NaCl	Roth	Cat#9265.2
$NaHCO_3$	Roth	Cat#8551.2

(*Continued on next page*)

REAGENT or RESOURCE	SOURCE	IDENTIFIER
Continued		
KCl	Roth	Cat#6781.2
NaH_2PO_4	Roth	Cat#K300.2
D-glucose	Roth	Cat#6780.2
sucrose	Roth	Cat#4661.2
$MgCl_2$	Roth	Cat#HN03.3
$CaCl_2$	Roth	Cat#CN93.2
K-gluconate	Merck	Cat#P1847
EGTA	Roth	Cat#3054.3
Na_2-Phosphocreatine	Merck	Cat#P7936
HEPES	Roth	Cat#6763.2
Na_2-ATP	Merck	Cat#A7689
Na_2-GTP	Merck	Cat#G8877
TTX	Hello Bio	Cat#HB1035
CNQX	Hello Bio	Cat#HB0205
D-AP5	Hello Bio	Cat#HB0225
Picrotoxin	Merck	Cat# P1675
SR95531	Alomone	Cat#G-216
CGP 55485 A	Biotechne	Cat#1248
DAPI	Merck Sigma	Cat#D9542
Paraformalhehyde	Carl Roth	Cat#0335.3
Streptavidin, Alexa Fluor™ 594 Conjugate	Fisher Scientific	Cat#S11227
Alexa Fluor™ 594 Hydrazide	Fisher Scientific	Cat#A10438
Biocytin	Fisher Scientific	Cat#11594157
Experimental models: Organisms/strains		
Mouse strain: CD1/Swiss genetic background (8-10 weeks, males)	Janvier labs	Rj: SWISS; RRID:IMSR_RJ:SWISS
Software and algorithms		
Image J	Schneider et al., 2012	https://imagej.net RRID:SCR_003070
Imaris	Oxford Instruments Group	https://imaris.oxinst.com/packages RRID:SCR_007370
Mathematica 9,13	Wolfram	https://www.wolfram.com/mathematica RRID:SCR_014448
Graphpad Prism	GraphPad	https://www.graphpad.com RRID:SCR_002798
QuPath-0.5.1	QuPath	https://qupath.github.io RRID:SCR_018257
Minianalysis (version 6.0.7)	–	https://www.synaptosoft.com/MiniAnalysis (obsolete) RRID:SCR_002184
Stimfit 0.15	Guzman et al., 2014	https://github.com/neurodroid/stimfit RRID:SCR_016050
Other		
High-quality water Milli-Q Super Q	Merck Millipore	Ref. F4MN43789B
P-97/PC Pipette Puller	Sutter Instruments	https://www.sutter.com RRID:SCR_018636
Borosilicate glass (2 mm OD/1 mm ID)	Hilgenberg	Cat#1807524
Borosilicate θ glass (2 mm OD/1.4 mm ID)	Hilgenberg	Cat#1401046
Superfrost slides	Fisher Scientific	Epredia J1800AMNZ
Dodt-gadient contrast	Luigs&Neumann	Cat#200-100 200 0155
Axopatch 200B	Molecular devices	RRID:SCR_018866
DigiData 1440 digitizer	Molecular devices	RRID:SCR_021038
Filter candles with tube (large)	Robu	Cat#AL-18124
Filter candles with tube (small)	Robu	Cat#AL-18104
VT-1200 vibratome	Leica Microsystems	RRID:SCR_020243
Video graphic printer	Sony	UP-897 MD
Digital camera ORCA-Flash 4.0 LT3	Hamamatsu	Cat#C11440-42U40
Microscope Zeiss Axioskop FS	Carl Zeiss	Cat#451406
Water immersion objective 40X/0.75 NA Achroplan	Carl Zeiss	Cat#40 00 90
4-time filter changer	Luigs&Neumann	Cat#200-100 200 0159-10
Infrared filter	Luigs&Neumann	Cat#400-000 000 1015

(*Continued on next page*)

Continued

REAGENT or RESOURCE	SOURCE	IDENTIFIER
LN electrode bracket stabilization	Luigs&Neumann	Cat#200-100 500 0251-21
LN modified electrode bracket	Luigs&Neumann	Cat#200-100 500 0252-A
Digital Manometer	Sigmann Elektronik GmbH	Cat#90262020
Razor blade Gillette Platinum	Gillette	7702018519095
Razor blade Gillette SuperSilver	Gillette	GIN 642107
Micro forge Microgrinder MF-830	Narishige	RRID:SCR_022055
Isolated Current Stimulator	Digitimer	DS3
Magnetic holders	Eclipse magnetics	Cat#E802, E822
Liquid superglue („Sekundenkleber")	UHU	Cat#45570
Freezing point osmometer	Gonotec	Osmomat 3000 basic
Syringe driven filter unit Millex-GV 0.22 μm	Millipore	Cat#SLGVR04NL
Platinum blades for the slicer	Gilette	Id. Num. 07702018926923
Slice anchor	Harvard Bioscience/Warner Instruments	Cat#64-1418, SHD-41/15
Zeiss LSM 880 with Airyscan Confocal Laser Scanning Microscope	Carl Zeiss	RRID:SCR_020925
Polypropylene (PP) Griffin beaker (VITLAB GmbH)	Carl Roth	Cat#2876.1
Crystallizing dish with spout from Duran	Carl Roth	Cat#21 311 41 02 Carl Roth Cat. No. C095.1
Theta glass (borosilicate) for stimulation electrode	Hilgenberg	Cat#1401046
Long scissors, 150 mm	Aesculap; Braun SE	Cat#AESCBC325R
Short scissors, 120 mm	Aesculap; Braun SE	Cat#AESCBC064R

STEP-BY-STEP METHOD DETAILS

Preparation before cutting brain slices

Timing: 1 h 30 min

This step describes the solutions for cutting brain slices and the preparation of the vibratome.

1. Prepare the sucrose-based cutting solution.
   a. Fill two 400 mL polypropylene (PP) Griffin beakers (e.g., from Vitlab) with ~400 mL sucrose-based cutting solution.
   b. Place the beakers at −80°C for ~45 min.

   Note: Polypropylene beakers are thermostable and tolerate rapid cooling.

   c. Remove the beakers from the freezer.
   d. Scrape partially frozen solution from the beaker walls and homogenize the slurry to obtain an ice-cold, non-frozen solution.

   CRITICAL: The solution must be cold but fully liquid.

   e. Remove all solid ice fragments to avoid mechanical damage to the brain.
   f. Oxygenate the sucrose-based cutting solution with 95% O_2/5% CO_2 for at least 20 min before brain dissection.
2. Prepare the vibratome and all dissection instruments in advance (Figure 2A).
3. Place the mouse in an anesthesia chamber and pre-oxygenate with 100% O_2 for >10 min[33,35] before anesthesia induction.

   Note: Preoxygenation improves brain oxygenation and reduces ischemic damage during tissue extraction. Supply the animal with O_2 even when using injectable anesthetics.

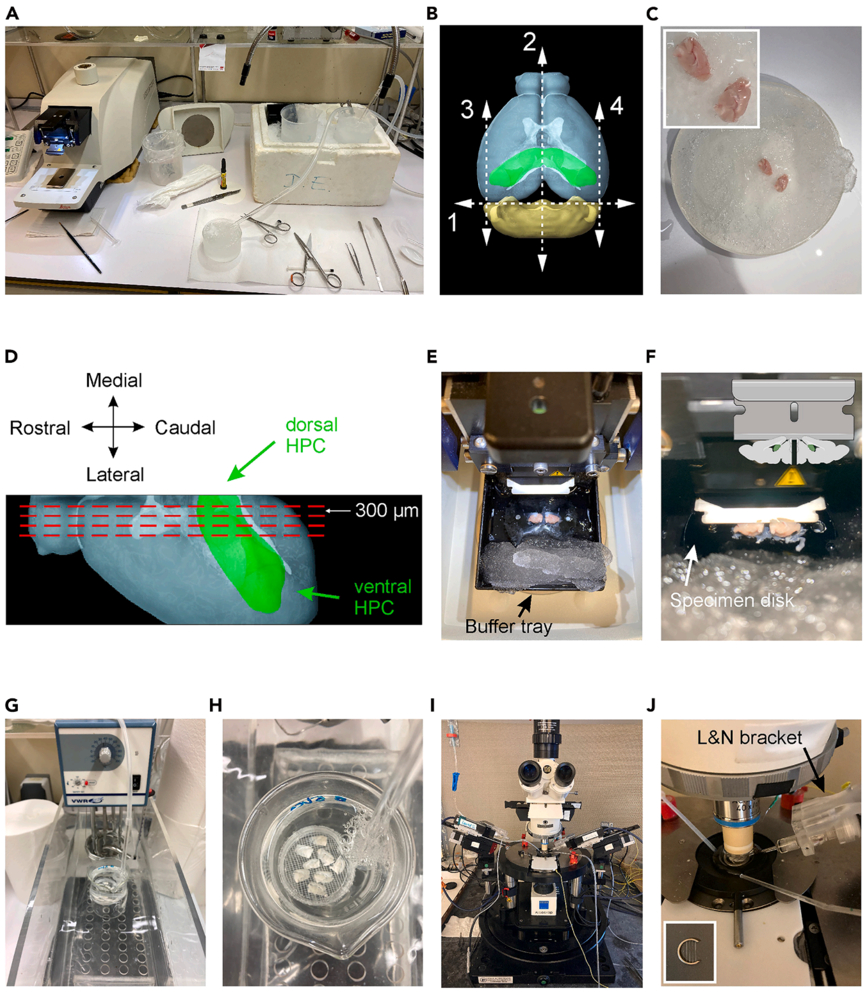

Figure 2. Patch-clamp recording system

(A) Overview of the preparation table showing the slicer at the left, two PP beakers on ice containing sucrose solution supplied with 95% O2 and 5% CO2. At the foreground a 80 mm in diameter crystallizing dish containing sucrose solution oxygenated using 95% O2 – 5% CO2 is to receive the brain after resection. Large scissors are to remove the head and small scissors to open the skull with a caudal to nasal cut.

(B) Schematic representation of the sequential cuts to prepare hemispheres. View of a mouse brain from the top. The cerebral cortex is in grey, the cerebellum in yellow and the hippocampal region in green. A first cut (1) using a scalpel is to remove the cerebellum. A second sagittal cut (2) is to separate both hemispheres. A third (3) and a fourth (4) cut are to remove a small piece of tissue at the lateral side of the hemispheres. The lateral side of the hemisphere is glued on the specimen disk. Three-dimensional structure of adult mouse from Brain Explorer 2 (version 2.3.5 Built 2393, Allen institute, https://brain-map.org).

(C) View of the medial side of the two hemispheres in a Petri dish after sagittal cut of the whole brain. The base of the Petri dish is filled with hardened agarose. Brain tissue is lying on the agarose layer and surrounded by liquid-solid sludgy sucrose solution. Inset shows an enlarged view of the hemispheres.

(D) View of the top of a mouse brain hemisphere. The brain is in gray and the hippocampus (HPC) in green. Parasagittal slices are cut starting from the medial side of the hemisphere towards the lateral side. Red dashed lines represent consecutive cuts to produce 300 µm thick slices containing the dorsal hippocampus (dorsal HPC). Three-dimensional structure of adult mouse from Brain Explorer 2 (version 2.3.5 Built 2393, Allen institute, https://brain-map.org).

(E) Cutting of brain slices in the parasagittal plane using the vibratome. View of the buffer tray containing sucrose solution with a liquid phase close to the hemispheres and a liquid-solid sludgy phase at the border of the buffer tray.

(F) Magnified view of the buffer tray. Hemispheres are glued on a specimen disk. The specimen disk contains a magnet in order to be maintained at the bottom of the buffer tray. Inset shows a scheme representing a blade cutting sagittal slices. The brain is in gray and the hippocampus in green. The scheme was created in Biorender.

(G) Overview of the water bath containing the storage chamber enclosing the brain slices. Tissue is maintained at a temperature of 34°C.

Figure 2. *Continued*

(H) Top view of a storage chamber filled with sucrose solution. A gauze net maintains slices at ~half-height of the beaker. A small micro filter candle supplies 95% O2 and 5% CO2 gas mixture to the solution. Very small gas bubbles are delivered by micro filter candles with a porosity of 4 corresponding to small pores.
(I) Front view of the patch-clamp setup. The microscope is mounted on a table allowing movement in the two horizontal X-Y directions. Manipulators to move pipette are left and right to the recording table. An optical 4-time filter changer (Luigs&Neumann) containing magnification glasses is mounted on the top of the microscope and the digital camera (not appearing in the overview) on top of optic changer.
(J) Recording chamber containing a brain slice. A water immersion objective (40X) is on top of the slice to visualize neurons. At the right a patch pipette in a pipette holder (Luigs&Neumann) with a bracket (Luigs&Neumann) surrounding the pipette holder to stabilize pipette. Inset shows the stainless steel slice hold-down flat frame with threads (Warner Instruments).

4. Prepare a 9 cm Petri dish with a ~5 mm layer of agar at the bottom (Figure 2C).

    Note: This dish will be used to section the brain into hemispheres immediately after extraction.

Brain slice preparation

Timing: 30 min

This step describes the procedure to obtain living brain tissue.

5. Dissect the brain.
    a. Anesthetize the mouse using isoflurane (3%–4% in 100% O_2).
    b. Decapitate the mouse using long (150 mm, Aesculap, cat. No. AESCBC325R) scissors.

    Note: Decapitation is a classical method of euthanasia.

    c. Remove the skin.
    d. Open the skull from caudal to rostral with short (120 mm, Aesculap, cat. No. AESCBC064R) scissors.
    e. Remove both half parts of the skull using forceps from the center of the head to the lateral side.

    ⚠ CRITICAL: Take care to cut the dura mater, the connecting tissue between skull and brain, to avoid damage at the surface of the hemispheres.

    f. Rapidly remove the brain using a spatula and immediately transfer it into ice-cold (0°C–4°C), oxygenated sucrose solution for a couple of minutes.

    ⚠ CRITICAL: Minimize the time between decapitation and immersion in cutting solution (<10 s whenever possible[42]). The quality of the slices is critically dependent on rapidity of this step.[20]

6. Separate the hemispheres.
    a. In a 9 cm diameter petri dish covered with agar, bisect the brain into two hemispheres using a mid-sagittal cut (dashed line 2) with a scalpel (Figures 2B and 2C).

    ⚠ CRITICAL: During this procedure, the brain must be completely submerged in the sucrose solution.

    b. Perform a cut using a scalpel in the parasagittal plane at the lateral side of the hemispheres as illustrated by the dashed lines 3 and 4 in Figure 2B.

Note: The resulting hemispheres are in Figure 2C.

7. Glue each hemisphere onto the specimen disk with the lateral surface facing downward.

   Note: The surface of the specimen disk must be absolutely dry. We recommend the cyanoacrylate superglue UHU "Sekundenkleber"[20,26] to adhere the brain tissue onto the specimen disk. Coat the specimen disk with a thin layer of superglue[20] in order to cover an area of ~1 cm^2.

8. Once the hemispheres are secure, pour sucrose solution on the top of the tissue block with a Pasteur pipette.

   Note: The flow of solution will hydrate the tissue and remove the glue from the lateral sides of the brain tissue blocks.

9. Place the specimen disk in the buffer tray.
10. Immediately pour sucrose ACSF into the buffer tray and fill it to ensure the hemispheres are fully submerged.
11. Prepare sagittal slices of the hippocampus.
    a. Cut 300 μm thick sagittal slices by advancing the blade from medial to lateral.

    Note: We use a Leica VT-1200 vibratome (Figures 2D–2F). Alternatively, use the stable Dosaka (DTK-1000, Kyoto, Japan),[43] the DTK-Zero 1 or the 7000smz-2 (Campden Instruments). To record from neurons in the dorsal hippocampal CA2 region,[7,8,12,19] we recommend sagittal slices (Figure 2D) as in refs.[6–8]

    b. Use the following[44] settings for the movement of the blade in the vibratome (Leica VT-1200):
    c. Blade oscillation amplitude of 1.20 mm.
    d. Blade forward movement velocity of 0.05 mm sec^{-1}.
    e. Use Gillette platinum or Gillette SuperSilver[26] blades.

    Note: All the utensils, tools and containers in contact with the tissue (e.g., forceps, scissors, blade) must be very clean[45] and rinsed using double distilled water. Metal utensils should be washed using double distilled water and passed through an oven (200°C/2 h). High degree of cleanliness of utensils helps to maintain brain slice healthy.[45]

    ⚠ CRITICAL: Separate carefully equipment, beakers and utensils (Pasteur pipettes) in use at the patch-clamp setup from those in contact with fixative.[20]

    f. Transfer slices to a storage chamber containing ACSF equilibrated with 95% O_2–5% CO_2 (pH=7.4) using a glass Pasteur pipette (via the wide end).
    g. Select slices in which the hippocampal formation is clearly identifiable by eye.
    h. Once all slices have been transferred to the storage chamber, incubate them at 33°C for 30 min (Figures 2G and 2H).
    i. Subsequently, maintain the storage chamber at room temperature (20°C–25°C).
    j. Allow slices to rest for at least 20 min before transfer to the recording chamber.

Patch-clamp recording

⏱ Timing: 4–6 h

This step uses the patch-clamp technique to achieve current- and voltage recordings from CA2 neurons.

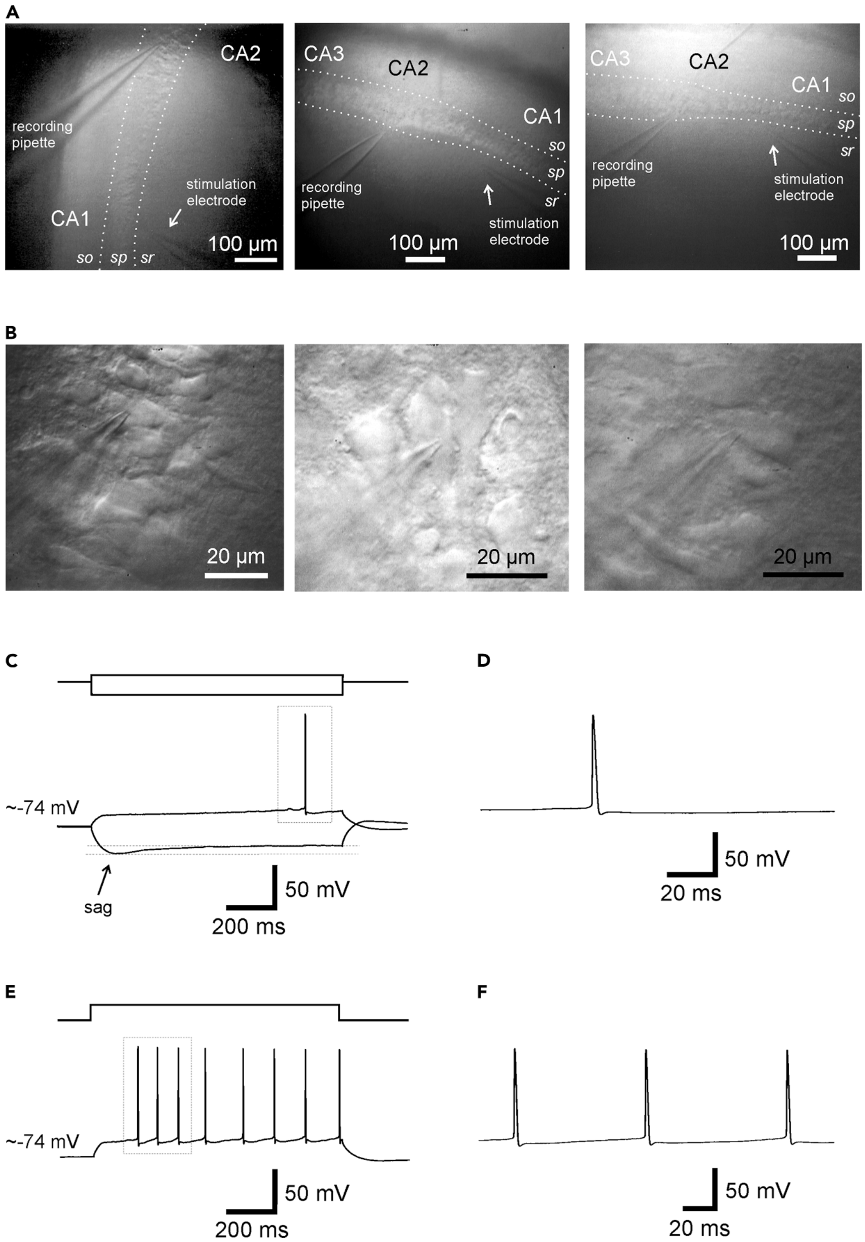

Figure 3. Patch-clamp recording in the CA2 region of the hippocampus

(A) Infrared (IR)-Dodt gradient contrast (DGC) images from three distinct experiments at low magnification (5X objective) showing a patch-clamp pipette during a whole-cell recording of a CA2 pyramidal neurons. sp is stratum pyramidale, sr stratum radiatum and so stratum oriens. Note the thicker pyramidal cell layer of CA2 in comparison to the pyramidal cell layer of CA1. Place a stimulation electrode in the stratum radiatum (sr) of CA1 where afferent fibers to CA2 run to generate electrically evoked synaptic events.

(B) IR-DGC high magnification images (40X objective) from three different experiments presenting a patch pipette during the recording of a CA2 pyramidal neuron. Note the triangular (pyramidal) shape of CA2 pyramidal neurons.

(C) Voltage traces (bottom) evoked by 1 sec long current injections of −200 pA (low) and +100 pA (top) in a putative CA2 pyramidal neuron. Note the presence of a small membrane potential rectification (sag) at the beginning of the voltage trace obtained with the hyperpolarizing current injection. The amplitude of the sag can be measured between the two dashed light gray lines.

(D) Enlargement of the top voltage trace (dashed gray square in C) showing the time course of the action potential obtained with +100 pA current pulse.

(E) Voltage traces evoked by 1 sec long current injections of +150 pA in the same neuron as in C.

Figure 3. ***Continued***

(F) Enlargement of a segment of the voltage trace (dashed gray square in E). Note the presence of a fast hyperpolarizing potential and the absence of a prominent slow afterhyperpolarization during the hyperpolarizing phase of action potentials. Resting membrane potential in this neuron is −74 mV, capacitance ~110 pF and input resistance 134 MΩ (measured using I-V curve).

12. Transfer a slice from the storage chamber to the recording chamber.
    a. Transfer one slice into the recording chamber using a Pasteur pipette (Figure 2I).
    b. Secure the slice with a platinum ring[22] or slice anchor at the bottom of the recording chamber[29] (Figure 2J).
    c. Continuously perfuse with ACSF.

Note: Ensure the slice remains fully submerged.

13. Select a CA2 neuron.
    a. Using a low magnification objective (5X), identify the characteristic hippocampal formation (Figure 3A).
    b. Locate the *stratum pyramidale* (*sp*) of CA3 and CA1, then focus on the *sp* between these subfields.

    Note: At this location is the also the distal end of the *stratum lucidum* (*sl*, between *sp* and *stratum radiatum* [*sr*]).

    c. Under high magnification (40X) with DIC of Dodt optics, identify CA2 by its thicker pyramidal cell layer (*sp*) compared with CA1[7,12,16] (Figure 3B).
    d. Identify if possible large mossy fiber boutons in the *sl* of CA3 (Figure 2 in ref;[20] and Figure 1 in ref;[46]) which should no longer be present in *sr* of CA2.[47]
    e. Select a neuron with a large pyramidal cell body, similar to CA3 neurons and larger than those in CA1[47,48] (Figure 3B).
14. Position patch pipette.
    a. Back-fill a recording pipette with internal solution.
    b. Mount it in the electrode holder.
    c. Apply positive pressure (60–70 mbar) using tubing connected to the electrode holder.

    Note: Apply pressure by mouth,

    d. Control the amount of pressure using a manometer (e.g., Pro D01 [Senseca Germany GmbH], or digital manometer [Sigmann Elektronik GmbH, Germany] or pressure manometer [WPI]).
    e. Maintain the pressure using a 3-way tube connector (https://swharden.com/patch/crash/how/) to prevent debris from entering and clogging the pipette tip.
15. Enter in the whole-cell configuration.
    a. Select a pyramidal neuron in CA2 with a smooth membrane surface (Figure 2 in ref.[49]) using a high magnification objective (Figure 3B).
    b. Using a low-drift 3-axis manipulator (e.g., L&N 25 Mini), position the pipette tip 2–5 µm from the neuronal membrane such as in Figure 4 (ref.[25]).

    Note: The pipette tip should come into contact with the neuron represented as a ball at 45° latitude.[20]

    c. Maintain positive pressure (60–70 mbar) until a slight membrane dimple is be observed, indicating close contact with the cell surface.

    Note: This dimple is a small invagination of the membrane around the pipette tip which appears in reaction of the cell's membrane to the positive pressure.

d. Once the dimple is clearly visualized (see Figure 2A in ref[26] or https://swharden.com/patch/crash/how) release the pressure.
e. Apply brief negative pressure using mouth to form a high-resistance seal (largely >1 GΩ).

Note: This configuration corresponds to the cell-attached mode.[22,50]

f. After seal stabilization, apply additional negative pressure (suction with the mouth) to rupture the membrane under the pipette tip and to enter into the whole-cell configuration.

Note: To facilitate membrane rupture, use the zap function implemented in the amplifier. Zap generates a large hyperpolarizing voltage (1.3 VDC for a chosen duration) causing dielectric breakdown of the membrane (Axon Axopatch 200B Microelectrode Amplifier manual and ref.[22]). A practical example to establish a whole-cell recording is in: https://swharden.com/patch/crash/how.

g. Immediately after break in, switch to current-clamp (I=0).
h. Record the resting membrane potential.
i. Switch to current-clamp (CC fast).
j. Record the firing of the neuron in whole-cell configuration using applications of increasing current steps (Figures 3C–3F).
k. Switch back to voltage-clamp.
l. Note the values for membrane potential (∼−75 mV), input resistance (∼76 MΩ) and capacitance (∼300 pF) that are directly reported by the acquisition software and compare them with the corresponding values from previous reports.[6,16,19]

⚠ CRITICAL: Discard immediately recordings with resting membrane potential more depolarized than −50 mV.[26]

m. Monitor and record systematically the passive (capacitive and leakage) currents by applying a 5 mV, 100 ms voltage step in voltage-clamp.

Note: The maximal amplitude of the capacitive current is indicative of the series resistance ($R_s = U_{step}/I_{cap}$, Figures 4A and 4B). The amplifier software gives also directly the value of the R_s.

n. Try to obtain the lowest possible R_s by applying negative pressure to the pipette tip. o. Read the amplitude of the capacitive current using a 10 kHz low pass filter.

⚠ CRITICAL: Discard recordings with series resistance R_s >10 MΩ. Check routinely the R_s during and at the end of the recording, the value of which should be stable within 10% (Figure 4B).

o. Sample the current using appropriate digitalization frequency (at least three times the filter cutoff frequency) considering Nyquist theorem (The Axon guide and ref.[22]). For example, sample a current at 50 kHz when using a filter of 10 kHz.
p. Abort recording if the firing pattern of the neuron does not correspond to the typical firing of a CA2 pyramidal neuron (Figures 3C–3F).

16. Record synaptic events.
    a. Record synaptic currents in whole-cell voltage-clamp for several minutes per condition.
    b. Use a low pass filter of 5 kHz.
    c. For mIPSCs,[51] add CNQX (10 μM) to block AMPA receptors, D-AP5 (20 μM) to block NMDA receptors and 1 μM tetrodotoxin to block voltage-gated Na^+ channels[52] to the ACSF (Figures 5A–5D). Additionally, use a KCl-based internal solution in the patch pipettes (Table 3).

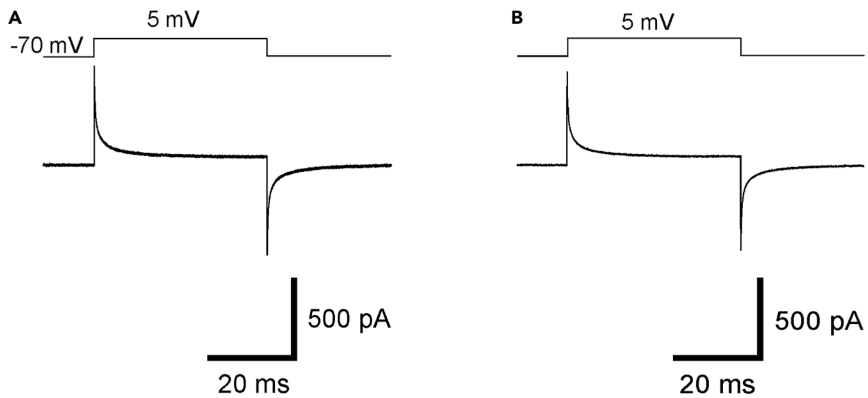

Figure 4. Passive properties of CA2 pyramidal neurons and miniature IPSCs

(A) Capacitive and leakage currents in a CA2 pyramidal neuron in response to a 5 mV voltage step recorded at a holding potential of Vh=−70 mV before the current trace in Figure 5A. The series resistance Rs is 8.1 MΩ. Capacitive transients are fitted with the sum of two exponentials giving time constants of 30 and 355 pF. Read out value from clampEx was Cm=210 pF. Current trace is an average of 9 raw traces.

(B) Capacitive and leakage currents acquired after the current trace in C to show the absence of gross change in the passive properties of the cell and recording conditions. Rs is 8.8 MΩ (less than 9% change in comparison to condition in A). Average current trace from 11 raw traces. Current traces in A and B are recorded in the presence of 20 μM D-AP5, 10 μM CNQX, and 1 μM TTX.

d. For spontaneous EPSCs (sEPSCs), add picrotoxin (50 μM) to the ACSF (Figures 5E–5H). In addition, fill patch pipettes with a K-gluconate internal solution (Table 4).

Note: Record IPSCs and EPSCs in separate slices to avoid pharmacological carryover.

⚠ CRITICAL: Abort recording if holding current is larger than −130 pA.[1,52]

e. To examine the EPSP-IPSP sequence, fill the recording electrode with a K-gluconate based pipette solution (Table 5).
f. Place a θ-glass stimulation electrode filled with Na^+-rich solution (Table 6) in CA1 *stratum radiatum* (*sr*) to evoke synaptic potentials[7,16,53] in CA2 pyramidal neurons (Figures 6A and 6B).
g. Connect the stimulation electrode to a constant current isolated stimulation unit (e.g., DS3 [Digitimer], ISO-Flex [AMPI], ISO-STIM-II [npi]).
h. Stimulate at low frequencies (0.05–0.1 Hz) to minimize synaptic rundown.
i. Document the recorded neuron (Figure 3B) using a thermal video printer connected to an infrared sensitive camera (e.g., NC-70 Newvicon, Dage-MTI)[1] or a digital frame grabber (image acquisition software with the digital camera, for example Hamamatsu ORCA Flash 4.0).

17. Terminate whole-cell recording.
    a. At the end of the recording, gently retract the pipette to form an outside-out patch[21,22] in order to promote membrane resealing.

Note: This procedure allows with a high probability the proper closing of membrane from the recorded neuron. The outside-out patch will not be further used but achieving an outside-out patch without leakage current hints to a proper closing of the cell membrane. The closing of the cell membrane is critical to preserve the intracellular milieu and the biocytin necessary for post hoc identification of the recorded neuron.

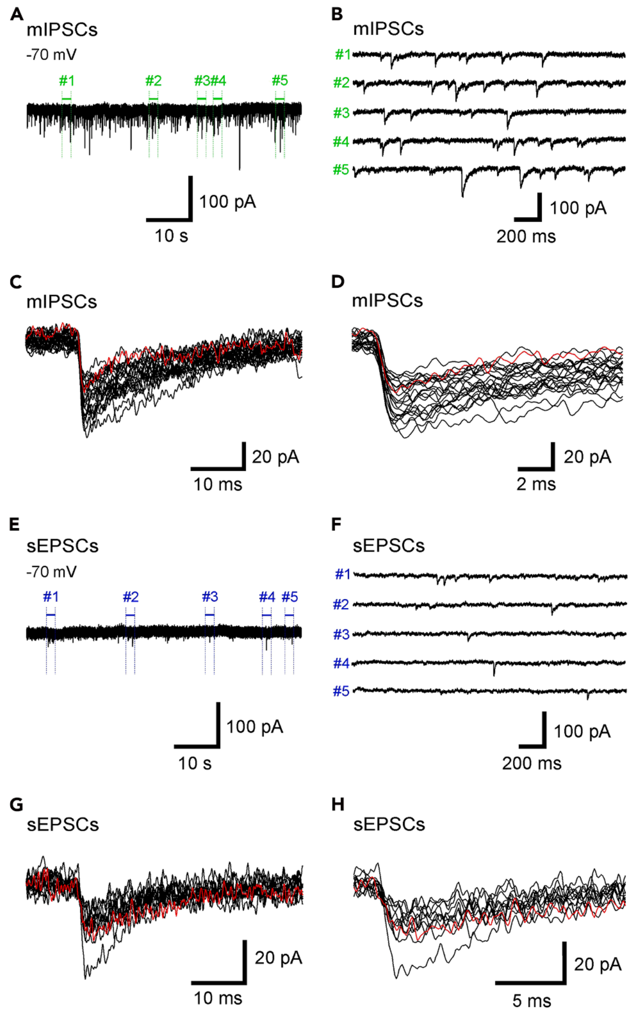

Figure 5. Excitatory and inhibitory spontaneous synaptic currents in CA2 pyramidal neurons

(A) Representative recording of mIPSCs at a holding potential of Vh=−70 mV. 20 μM D-AP5, 10 μM CNQX, and 1 μM TTX are added to external solution to block excitatory synaptic activity and spontaneous AP firing. Green dashed vertical lines indicate the sections of current selected for expanded time view in B. Current trace sections are labeled #1 to #5.

(B) Selection of five current trace sections extracted from current trace in (C).

(C) Miniature currents selected using Clampfit with template matching selection method. Superimposition of 23 individual current traces in black with one in red.

(D) Current traces from (C) at expanded time scale.

(E) Original trace of sEPSCs recorded at a holding potential of Vh=−70 mV. 50 μM picrotoxin was added to external solution to block inhibitory synaptic activity. Blue dashed vertical lines indicate the sections of current selected for expanded time view in F.

(F) Five current trace segments (blue label #1 to #5) extracted from the whole current trace in (E) at expanded time scale.

(G) Spontaneous excitatory postsynaptic currents selected using Clampfit with template matching selection method. Superimposition of 12 individual current traces in black with one in red.

(H) Current traces from (G) at expanded time scale.

b. Retract the pipette using sequential lateral-upward very slow movement.[20]
c. After pipette withdrawal, maintain the slice in the recording chamber for an additional 30 min to allow biocytin to reach uniformly the entire neuron until the extremity of the dendrites.[20,26]
d. Replace the slice after each completed recording.

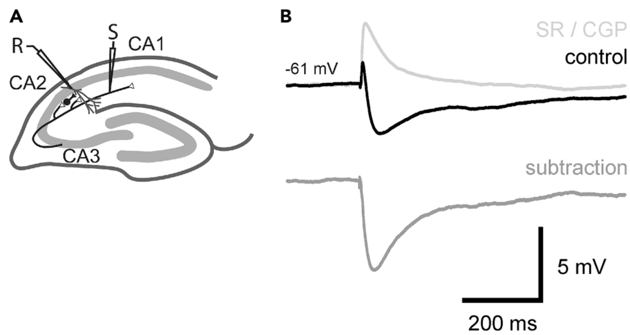

Figure 6. Feedforward inhibition in CA2 pyramidal neurons

(A) Scheme representing the experimental protocol to record a EPSP/IPSP sequence in a CA2 pyramidal neuron. Schaffer collaterals are stimulated using the pipette (S) to depolarize axons originating from CA3. The recording electrode (R) is on a CA2 pyramidal neuron. Scheme adapted from ref.[53]

(B) Voltage traces of a EPSP/IPSP sequence (control, black trace), an EPSP after GABAA and GABAB receptor blockade (10 μM SR95531 and 1 μM CGP 55485A, light grey) and the subtracted IPSP (grey) recorded in a CA2 pyramidal neuron in response to Schaffer collaterals stimulation. Stimulation strength (40–100 μA; 100 μs duration) is adjusted to evoke baseline component EPSPs with amplitudes of 1–4 mV. EPSPs are recorded using a stimulation frequency of 0.2 Hz. Potential is held at Vm∼−61 mV.

Biocytin labeling of the recorded neuron and immunohistochemical labeling of the hippocampal CA2 subfield

Timing: 2 h distributed over 3 days

This step indicates the procedure to determine the position of the recorded cell in the slice and to identify the surrounding subfield.

18. Fix slices.
    a. Immediately after completion of the electrophysiological recording, transfer slices to 4% paraformaldehyde (PFA) prepared in 0.1 M phosphate buffer saline (PBS; pH 7.4) overnight (at least 8 h) at 4°C.
    b. After one night in fixative, rinse the slices 3 × 5 min at room temperature (RT, 20°C–25°C) using 0.1 M PBS.
19. Incubate slices with primary and secondary antibodies.
    a. Incubate with the primary antibody from the mouse, anti-RGS14 (1/500, overnight at RT), in PBS containing 0.1% triton.

Note: RGS14 is the abbreviation of Regulator of G-protein Signaling 14.

    b. Rinse 3 × 5 min in PBS 0.1 M at RT.
    c. Incubate at RT with the secondary antibody anti-mouse (coupled to a fluorochrome [e.g., Alexa Fluor 647]) to recognize the primary antibody and with streptavidin-Alexa Fluor™ 594 Conjugate (1 μl) in PBS 0.1 M containing 0.1% triton.

Note: Biocytin contained in the recorded neuron is revealed using for example streptavidin conjugated to Alexa 564.

    d. Rinse 3 × 5 min the slices using PBS 0.1 M (RT).

Note: Protect samples from light from this step onward.

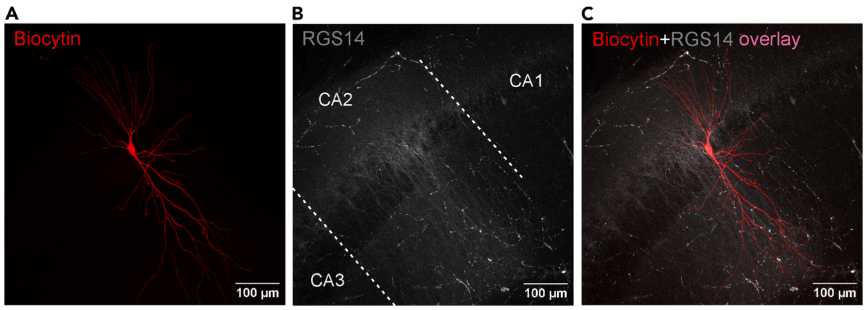

Figure 7. Pyramidal neuron in the hippocampal CA2 subfield

(A) Confocal light-micrograph of a biocytin-filled pyramidal neuron stained with Alexa 564 conjugated streptavidin.

(B) Labeling of RGS14 immunoreactivity using Alexa 647. Dashed white lines indicate approximative proximal-distal boundaries of CA2.

(C) Overlay of biocytin and RGS14 labeling. Note the presence of recorded pyramidal neuron in the CA2 stained subfield.

20. Mount the slices on microscope slides (Superfrost slides, Fisher Scientific, Epredia J1800AMNZ) using mounting medium (Fluoromount aqueous medium, Sigma-Aldrich, Cat. No. F4680).
21. Examine labeling using a confocal microscope.
    a. Locate the biocytin-labeled neuron within the hippocampal CA2 subfield labelled using a specific marker (e.g., RGS14) (Figures 7A–7C).

Note: The staining of the biocytin-filled neuron overlaps with the staining of the CA2 molecular marker (RGS14).

    b. Consider other markers for the CA2 subfield, such as the plant lectin Wisteria Floribunda agglutinin (WFA) to label the specialized extracellular matrix called perineuronal nets (PNNs),[18,54] or antibodies against PCP4 (Purkinje Cell Protein 4)[6,15,19,55] or antibodies against α-actinin.[6,7,16]

Note: Particularly, the overlap of WFA and PCP4 at the CA2/CA1 border is precise and indicates the transition between CA2 and CA1 which coincides with the transition between loosely packed nuclei and densely packed nuclei in CA1 as revealed by DAPI nuclear staining (Figures 8A and 8B). The labeling of WFA is stronger at the distal part than at the proximal part of CA2 as reported by ref.[18]

EXPECTED OUTCOMES

Despite the absence of clear anatomical landmarks, this protocol enables reliable selection of pyramidal neurons for whole-cell recordings within the hippocampal CA2. The vast majority of recorded neurons express established CA2 molecular markers, as previously validated.[1] In current-clamp, CA2 pyramidal neurons typically exhibit a delay to the first spike, minimal voltage sag, and absence of a slow after-hyperpolarization (Figure 3) in response to low-amplitude current injections, as reported by others.[6,16,19,56] Recorded neurons display robust spontaneous excitatory and inhibitory synaptic activity (Figures 5 and 6), enabling assessment of excitation-inhibition balance. With minor adaptations, this protocol can also be applied to other CA2 cell types, including interneurons[56] or even astrocytes.[57] Finally, biocytin-filling enables post hoc morphological analysis of recorded neurons, including soma size and the presence of thorny excrescences.[47]

QUANTIFICATION AND STATISTICAL ANALYSIS

Electrophysiological analysis

Electrophysiological parameters are measured from stable recording periods. Measure series resistance and capacitance from current response to a 5 mV, 100 ms voltage step in voltage-clamp at

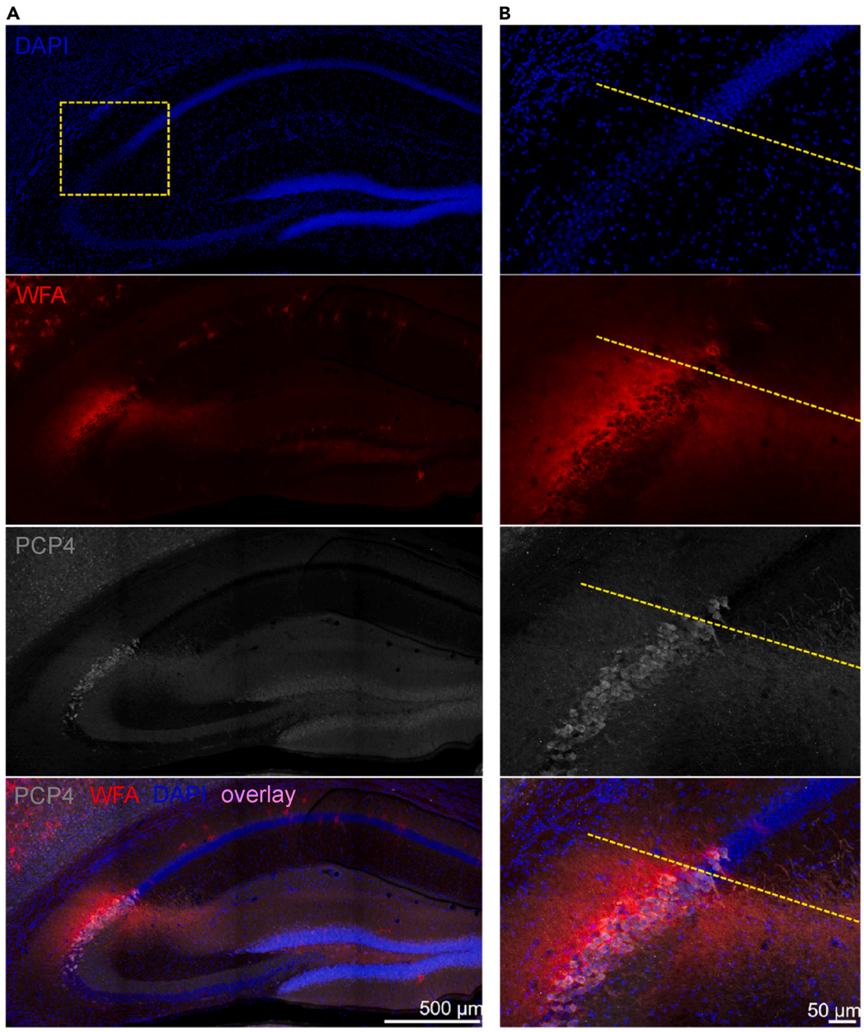

Figure 8. Identification of the hippocampal CA2 with specific regional markers

(A) Hippocampal cellular organization (DAPI, top in blue), expression of the putative CA2 markers WFA (second from the top in red) and PCP4 (third from the top in light grey) and overlay (bottom). Dotted yellow square is for enlarged views. WFA staining is revealed using Alexa 555 via biotin–streptavidin system conjugate and PCP4 staining using Alexa 647 via secondary antibody. Images are captured with a 63X oil objective mounted on a Zeiss LSM880 in Airyscan mode.

(B) Expanded view of the images in (A). The yellow dotted line represent the CA1/CA2 boundary. Note the clear transition in the distribution of the DAPI staining that coincides with the WFA and PCP4 staining and colocalization of WFA and PCP4 markers in CA2.

holding potential of V_h=−70 mV. Determine resting membrane potential in current-clamp immediately after whole-cell break-in in the absence of current injection (I=0). Calculate input resistance (R_{in}) from the slope of voltage-current relationship.[6,58] Calculate sag ratio as the ratio of peak to steady-state voltage deflection during hyperpolarizing current steps.[6] Analyze firing patterns from voltage responses to 1 s long current step injections of increasing amplitude (−200 pA, increment 50 pA). Analyze electrophysiological data using for example: Clampfit (Molecular devices), Stimfit,[59] Wolfram Mathematica, FITMASTER (HEKA), or Python (https://www.scientifica.uk.com/neurowire/patch-clamp-electrophysiology-analysis-with-python). Because Minianalysis software is no longer available, quantify synaptic event parameters (amplitude, rise time, decay time, frequency) using Clampfit[60] or Stimfit by using either template-based[52] or threshold-based methods to select spontaneous postsynaptic currents along a current trace (https://spikesandbursts.wordpress.com/2022/05/25/patch-clamp-clampfit-synaptic-events). Alternatively, use a deconvolution-based method.[61] Consider carefully the quality of each recorded current trace (regularity of the current trace and noise) and the event detection method to determine relevant synaptic currents in order to deliver appropriate data interpretation.[60] Include only synaptic events with fast rise times and smooth rising phase.[40] Perform statistical analyses using Excel, Prism or Wolfram Mathematica software. In CA2 pyramidal neurons, resting membrane potential V_m is ~-68.0 mV; input resistance R_{in} $\sim$92 mV; voltage sag $\sim$20 mV; capacitance $\sim$181 pF; action potential amplitude $\sim$93 mV and action potential threshold ~-46 mV as reported in ref.[1] Spontaneous IPSCs have an amplitude of $\sim$52 pA and a frequency of $\sim$5 Hz; mIPSCs an amplitude of $\sim$34 pA and a frequency of $\sim$3 Hz (from ref.[1]) and sEPSCs an amplitude of $\sim$16 pA and a frequency of $\sim$0.25 Hz.

Histological analysis

Acquire confocal images using Airyscan mode on a Zeiss LSM 880 or Zeiss LSM 980. Ensure reproducibility by performing immunohistochemistry experiments simultaneously and image analysis using the same imaging equipment and settings. Perform image analysis using Fiji (ImageJ) or QuPath (https://qupath.github.io).

Define the CA2 subfield based on the expression of PCP4 or RGS14.[62] These molecules are expressed by CA2 pyramidal neurons[17] and contribute to the regulation of specific cellular functions, such as synaptic plasticity.[12] To confirm that the recorded pyramidal neuron was located in CA2, we used RGS14 immunolabeling,[1] as this marker is more expressed in the dorsal hippocampus.[3,14]

Several molecular markers are used to delineate the CA2 region; however, recent evidence indicates that these proteins are not equivalent in their labeling properties.[18,62] RGS14 and PCP4 differ in their expression along the dorsal–ventral axis of the hippocampus, with RGS14 showing stronger expression in dorsal CA2 than in ventral CA2,[3] and PCP4 displaying a similar but weaker gradient.[13,14] Labeling of perineuronal nets (PNNs) with WFA is more intense at the distal part of CA2 (CA2/CA1 border) than at the proximal part of CA2 (CA2/CA3 border), particularly in ventral CA2.[18]

LIMITATIONS

This protocol is optimized for whole-cell patch-clamp recordings from healthy acute hippocampal slices and is derived from established methods[20] adapted for adult mouse tissue.[33,35] A major limitation of this technique is the substantial training required to achieve reliable results. Rapid brain extraction[20] is critical and should be completed within 30 s,[45] ideally within 10 s.[42] The dexterity of the operator influences therefore the quality of the slice preparation. Solid understanding of cellular electrophysiology is demanded during live recordings and for correct data interpretation. Neuron's health in terms of intrinsic excitability and synaptic connectivity must be preserved in slices in order to collect accurate data. The borders of the CA2 subfield (CA3/CA2 border and CA2/CA1 border) are not directly visible in slices under Dodt/DIC optics. Therefore, CA2 identity must be confirmed post hoc using immunohistochemical labeling.

Another limitation is the unavoidable tissue damage caused by slicing. Superficial neurons may have portions of their dendritic arbor or axon transected, leading to alterations in their electrophysiological properties. In addition, synaptic innervation can be severed, directly affecting the frequency of spontaneous synaptic currents. Therefore, neurons located deeper within the slice should be selected, despite the reduced visibility of the cell membrane.

TROUBLESHOOTING

Problem 1

Unhealthy neurons near the surface of brain slices (Brain slice preparation, steps 5–11).

Two common morphologies indicate unhealthy or dead neurons. The first type is characterized by a swollen, round, pale and transparent soma and a visible, swollen and contrasted nucleus (Figure 1 in ref;[31], Figures 2B–2E in ref.[23] and Figure 2B in ref;[49]). The second type by a strongly contrasted soma (Figure 2G in ref.[23] and https://swharden.com/patch/crash/how/). Recordings from these two types of neurons are unreliable and should be avoided. During these recordings, a high leakage current (>100 pA) is observed in whole-cell between the pipette and the cell membrane indicating the absence of a tight seal and/or membrane potential is too depolarized (>−50 mV).

Potential solution

- Thoroughly clean all utensils, tubing, glass beakers and chambers contacting tissue.
- Verify osmolarity of sucrose solution and ACSF before the experiment. The osmolarity values must be very close to the calculated values, ~326 and ~316 mOsm, respectively.
- Replace storage chamber. The degree of cleanliness of the inside of the storage chamber must be very high since slices rest in there for several hours.
- Prepare new slices from a second animal. Ensure that the resection of the brain and the placement of the organ in ice-cold sucrose solution is the fastest possible. Avoid to damage the brain with the dissecting instruments. Glue very quickly the hemisphere(s) on the specimen disk. Reduce exposure of the brain to the air and ensure the organ is surrounded by sucrose solution during the preparation time. These steps are critical to have living neurons.
- Ensure high-purity water (resistivity ≥18 mΩ·cm). The quality of the water used to prepare all the solutions must be very pure in order to obtain adequate osmolarity. Resistivity (which should be as high as possible) of the water gives an indication about the purity of the water.

Problem 2

Failure to achieve a >1 GΩ seal (Patch-clamp recording, steps 13–15).

Potential solution

- Target neurons 10–50 μm below the slice surface.[20,26,45]
- Avoid excessive positive pressure (>70 mbar) to the pipette tip because this may damage the membrane of the neuron.
- Inspect each pipette tip using the binocular loupes mounted on the microforge. Ensure pipette tip is clean and smooth and devoid of dust or dirt.
- Heat-polish the pipette tip using the microforge. Optimal heat-polishing is achieved with fast (1 sec) heating the filament.[20] Details for heat-polishing are in ref.[22] Coat the heating filament of the microforge with a small piece of pipette glass shard. This coating avoid an overheating of the filament.
- Select neurons with smooth, low-contrast membranes.

Problem 3

Non-CA2 pyramidal neuron firing pattern (Patch-clamp recording, step 13–15).

A typical firing is in Figures 3C–3F and in Figure 1 in ref.,[6,16,63] in Figure 2 in ref.[56] and in Figure 3 in ref.[19] CA2 pyramidal neurons display a late firing after a slow depolarization and an absence of a large afterhyperpolarization after the action potential in response to a positive current step injection. The amplitude of the sag in response to a hyperpolarizing current step is very small.[6,16,19]

Potential solution

- Abort the recording and select another neuron located in the putative CA2 subfield with respect to the criteria presented in the protocol (Figures 3A and 3B).
- Replace the slice and reassess CA2 location based on *stratum pyramidale* thickness.

Problem 4

Failure to evoke EPSPs in CA2 pyramidal neurons (Patch-clamp recording, step 16).

Potential solution

- Reposition the stimulation electrode within CA1 *stratum radiatum* close to *stratum pyramidale*. Move the electrode back and forth, or to the left or to the right until an EPSP is visualized using high current intensities (100 μA) and longer steps (1 ms). Move the electrode deeper under the surface of the slice to reach fibers that are not damaged. Move the stimulating electrode closer (~200–300 μm) to the recorded neuron.
- Target neurons deeper (40–60 μm) under the surface of the slice. Neurons from the surface may receive low synaptic input due to damaged axons.

Problem 5

Absence of biocytin-labelling (Internal pipette solutions).

Potential solution

- Ensure proper membrane resealing (outside-out formation).[20,26,50] Successful formation of an outside-out patch is characterized by an increase in seal resistance back into the GΩ range and a decrease in background noise following retraction of the pipette from the cell.[50]
- Increase biocytin concentration (from 1 or 2 mg/mL to 5 mg/mL) dissolved in the internal solution.
- Avoid CsCl-only internal solutions if biocytin labelling is necessary. Incorporate a gluconate conjugate (K-gluconate or Cs-gluconate) in the internal solution. CsCl can compromise the labelling of biocytin.[26]
- Pull pipettes with 3–4 MΩ resistance. Pipettes with high resistance >6 MΩ may cause insufficient diffusion of biocytin contained in pipette internal solution.
- Extend recording duration (~1 h) to enhance diffusion of biocytin.
- Control the concentration of the avidin conjugate. Increase avidin conjugate concentration to 2 μl mL^{-1} and incubate it with the slices at least for one night.

Problem 6

Weak or absent CA2 marker staining.

Potential solution

- Determine the optimal dilution for the primary and for the second antibody with series of experiments using increasing concentrations of antibody. This calculation is important because it produces staining with high signal and low background. For more details: https://www.thermofisher.com/be/en/home/life-science/protein-biology/protein-biology-learning-center/protein-biology-resource-library/pierce-protein-methods/ihc-troubleshooting-guide.html.
- Prioritize markers with strong dorsal CA2 expression (e.g., RGS14). Note that PCP4 is more widely expressed in pyramidal neurons from the ventral CA2.[3]

RESOURCE AVAILABILITY

Lead contact

Further information and requests for resources should be directed to and will be fulfilled by the lead contact, Laurent Nguyen (lnguyen@uliege.be).

Technical contact

Technical questions on executing this protocol should be directed to and will be answered by the technical contact, Dominique Engel (dominique.engel@uliege.be).

Materials availability

This study did not generate new unique reagents.

Data and code availability

This study did not generate new datasets or code. Source data for figures in the paper will be shared by the technical contact upon request.

ACKNOWLEDGMENTS

D.E. and L.N. are a Research Associate and a Research Director, respectively, at F.R.S.-F.N.R.S. We thank the members of the Nguyen lab for the discussion and feedback on the present work. We thank the GIGA imaging platform, and particularly Alexandre Hego, for helping with the acquisition of confocal images.

The work performed in the Nguyen laboratory is supported by ULiège (Crédit Classique de la faculté de médecine), the F.R.S.-F.N.R.S. (PDR T.0185.20 and EOS 0019118F-RG36), the WEL Research Institute(CR-2022A-12), the Fonds Leon Fredericq, the Fondation Simone et Pierre Clerdent, the Fondation Médicale Reine Elisabeth, the ERANET Neuron (STEM-MCD and NeuroTalk), the Win2Wal (ChipOmics, no. 2010126), and the ERC-Synergy(UNFOLD).

We thank Romain Le Bail for the immunohistochemical experiments shown in Figures 7 and 8. D.E. thanks Dr. Vivien Chevaleyre for his help in solving technical questions. First page illustration was created with https://BioRender.com.

AUTHOR CONTRIBUTIONS

Conceptualization, D.E. and L.N.; methodology, D.E.; writing – review and editing, D.E. and L.N.; funding acquisition, L.N. and D.E.

DECLARATION OF INTERESTS

The authors declare no competing interests.

REFERENCES

1. Le Bail, R., Lakaye, B., Espuny-Camacho, I., Janke, C., Magiera, M.M., Engel, D., Silva, C.G., and Nguyen, L. (2025). Ccp1 depletion disrupts network integration of hippocampal parvalbumin interneurons. iScience *28*, 113215. https://doi.org/10.1016/j.isci.2025.113215.

2. Bischofberger, J., Engel, D., Li, L., Geiger, J.R.P., and Jonas, P. (2006). Patch-clamp recording from mossy fiber terminals in hippocampal slices. Nat. Protoc. *1*, 2075–2081. https://doi.org/10.1038/nprot.2006.312.

3. Engel, D., and Jonas, P. (2005). Presynaptic action potential amplification by voltage-gated Na+ channels in hippocampal mossy fiber boutons. Neuron *45*, 405–417.

4. Lopez-Rojas, J., de Solis, C.A., Leroy, F., Kandel, E.R., and Siegelbaum, S.A. (2022). A direct lateral entorhinal cortex to hippocampal CA2 circuit conveys social information required for social memory. Neuron *110*, 1559–1572.e4. https://doi.org/10.1016/j.neuron.2022.01.028.

5. Boyle, L.M., Sheng, W., Villegas, A., Sahai, R., Irfan, S., Lee, H.-J., Young, W.S., Leroy, F., and Siegelbaum, S.A. (2025). The ventral CA2 region of the hippocampus and its differential contributions to social memory and social aggression. Cell Rep. *44*, 115714. https://doi.org/10.1016/j.celrep.2025.115714.

6. Oliva, A., Fernández-Ruiz, A., Buzsáki, G., and Berényi, A. (2016). Role of Hippocampal CA2 Region in Triggering Sharp-Wave Ripples. Neuron *91*, 1342–1355. https://doi.org/10.1016/j.neuron.2016.08.008.

7. Alexander, G.M., Farris, S., Pirone, J.R., Zheng, C., Colgin, L.L., and Dudek, S.M. (2016). Social and novel contexts modify hippocampal CA2 representations of space. Nat. Commun. *7*, 10300. https://doi.org/10.1038/ncomms10300.

8. Kohara, K., Pignatelli, M., Rivest, A.J., Jung, H.Y., Kitamura, T., Suh, J., Frank, D., Kajikawa, K., Mise, N., Obata, Y., et al. (2014). Cell type-specific genetic and optogenetic tools reveal hippocampal CA2 circuits. Nat. Neurosci. *17*, 269–279. https://doi.org/10.1038/nn.3614.

9. Chafai, M., Corbani, M., Guillon, G., and Desarménien, M.G. (2012). Vasopressin Inhibits LTP in the CA2 Mouse Hippocampal Area. PLoS One *7*, e49708. https://doi.org/10.1371/journal.pone.0049708.

10. Fernandez-Lamo, I., Gomez-Dominguez, D., Sanchez-Aguilera, A., Oliva, A., Morales, A.V., Valero, M., Cid, E., Berenyi, A., and Menendez de la Prida, L. (2019). Proximodistal Organization of the CA2 Hippocampal Area. Cell Rep. *26*, 1734–1746.e6. https://doi.org/10.1016/j.celrep.2019.01.060.

11. Skrede, K.K., and Westgaard, R.H. (1971). The transverse hippocampal slice: a well-defined cortical structure maintained in vitro. Brain Res. *35*, 589–593. https://doi.org/10.1016/0006-8993(71)90508-7.

12. Andersen, P., Morris, R., Amaral, D., Bliss, T., and O'Keefe, J. (2006). Chapter 3, Hippocampal Neuroanatomy. In The Hippocampus Book, P. Andersen, R. Morris, D. Amaral, T. Bliss, and J. O'Keefe, eds. (Oxford University Press). https://doi.org/10.1093/acprof:oso/9780195100273.001.0001.

13. Xiong, G., Metheny, H., Johnson, B.N., and Cohen, A.S. (2017). A Comparison of Different Slicing Planes in Preservation of Major Hippocampal Pathway Fibers in the Mouse. Front. Neuroanat. *11*, 107–117. https://doi.org/10.3389/fnana.2017.00107.

14. Dudek, S.M., Alexander, G.M., and Farris, S. (2016). Rediscovering area CA2: unique properties and functions. Nat. Rev. Neurosci. *17*, 89–102. https://doi.org/10.1038/nrn.2015.22.

15. Bienkowski, M.S. (2023). Further refining the boundaries of the hippocampus CA2 with gene expression and connectivity: Potential subregions and heterogeneous cell types. Hippocampus *33*, 150–160. https://doi.org/10.1002/hipo.23508.

16. Siegler, P.N., Shaughnessy, E.K., Horman, B., Vierling, T.T., King, D.H., Patisaul, H.B., Huhman, K.L., Alexander, G.M., and Dudek, S.M. (2024). Identification of hippocampal area CA2 in hamster and vole brain. J. Comp. Neurol. *532*, e25603–e25616. https://doi.org/10.1002/cne.25603.

17. Lein, E.S., Callaway, E.M., Albright, T.D., and Gage, F.H. (2005). Redefining the boundaries of the hippocampal CA2 subfield in the mouse using gene expression and 3-dimensional reconstruction. J. Comp. Neurol. *485*, 1–10. https://doi.org/10.1002/cne.20426.

18. Chevaleyre, V., and Siegelbaum, S.A. (2010). Strong CA2 pyramidal neuron synapses define a powerful disynaptic cortico-hippocampal loop. Neuron *66*, 560–572. https://doi.org/10.1016/j.neuron.2010.04.013.

19. Lee, S.E., Simons, S.B., Heldt, S.A., Zhao, M., Schroeder, J.P., Vellano, C.P., Cowan, D.P.,

Ramineni, S., Yates, C.K., Feng, Y., et al. (2010). RGS14 is a natural suppressor of both synaptic plasticity in CA2 neurons and hippocampal-based learning and memory. Proc. Natl. Acad. Sci. USA *107*, 16994–16998. https://doi.org/10.1073/pnas.1005362107.

20. Radzicki, D., Chong, S., and Dudek, S.M. (2023). Morphological and molecular markers of mouse area CA2 along the proximodistal and dorsoventral hippocampal axes. Hippocampus *33*, 133–149. https://doi.org/10.1002/hipo.23509.

21. Tirko, N.N., Eyring, K.W., Carcea, I., Mitre, M., Chao, M.V., Froemke, R.C., and Tsien, R.W. (2018). Oxytocin Transforms Firing Mode of CA2 Hippocampal Neurons. Neuron *100*, 593–608.e3. https://doi.org/10.1016/j.neuron.2018.09.008.

22. Sakmann, B., and Neher, E. (1995). Chapter 1, A Practical Guide to Patch Clamping. In Single-channel Recording, 2nd ed., B. Sakmann and E. Neher, eds. (Springer US). https://doi.org/10.1007/978-1-4419-1229-9.

23. Davie, J.T., Kole, M.H.P., Letzkus, J.J., Rancz, E.A., Spruston, N., Stuart, G.J., and Häusser, M. (2006). Dendritic patch-clamp recording. Nat. Protoc. *1*, 1235–1247. https://doi.org/10.1038/nprot.2006.164.

24. Roth, F.C., Numberger, M., and Draguhn, A. (2023). Patch-Clamp-Technik (Springer Berlin Heidelberg). https://doi.org/10.1007/978-3-662-66053-9.

25. Stuart, G.J., Dodt, H.U., and Sakmann, B. (1993). Patch-clamp recordings from the soma and dendrites of neurons in brain slices using infrared video microscopy. Pflugers Arch. *423*, 511–518. https://doi.org/10.1007/BF00374949.

26. Vandael, D., Okamoto, Y., Borges-Merjane, C., Vargas-Barroso, V., Suter, B.A., and Jonas, P. (2021). Subcellular patch-clamp techniques for single-bouton stimulation and simultaneous pre- and postsynaptic recording at cortical synapses. Nat. Protoc. *16*, 2947–2967. https://doi.org/10.1038/s41596-021-00526-0.

27. Dodt, H.-U., Schierloh, A., Eder, M., and Zieglgänsberger, W. (2003). Circuitry of rat barrel cortex investigated by infrared-guided laser stimulation. Neuroreport *14*, 623–627. https://doi.org/10.1097/00001756-200303240-00020.

28. Dodt, H.U., and Zieglgänsberger, W. (1990). Visualizing unstained neurons in living brain slices by infrared DIC-videomicroscopy. Brain Res. *537*, 333–336. https://doi.org/10.1016/0006-8993(90)90380-T.

29. Edwards, F.A., Konnerth, A., Sakmann, B., and Takahashi, T. (1989). A thin slice preparation for patch clamp recordings from neurones of the mammalian central nervous system. Pflugers Arch. *414*, 600–612. https://doi.org/10.1007/BF00580998.

30. Edwards, F.A., and Konnerth, A. (1992). Patch-clamping cells in sliced tissue preparations. In Methods in Enzymology, B. Rudy, ed. (Elsevier Inc), pp. 208–222.

31. Engel, D. (2016). Subcellular Patch-clamp Recordings from the Somatodendritic Domain of Nigral Dopamine Neurons. J. Vis. Exp. *117*, 54601–54616. https://doi.org/10.3791/54601.

32. Silva, C.G., Peyre, E., Adhikari, M.H., Tielens, S., Tanco, S., Van Damme, P., Magno, L., Krusy, N., Agirman, G., Magiera, M.M., et al. (2018). Cell-Intrinsic Control of Interneuron Migration Drives Cortical Morphogenesis. Cell *172*, 1063–1078.e19. https://doi.org/10.1016/j.cell.2018.01.031.

33. Schmidt-Hieber, C., and Bischofberger, J. (2010). Fast Sodium Channel Gating Supports Localized and Efficient Axonal Action Potential Initiation. J. Neurosci. *30*, 10233–10242. https://doi.org/10.1523/JNEUROSCI.6335-09.2010.

34. Geiger, J.R.P., Bischofberger, J., Vida, I., Fröbe, U., Pfitzinger, S., Weber, H.J., Haverkampf, K., and Jonas, P. (2002). Patch-clamp recording in brain slices with improved slicer technology. Pflugers Arch. *443*, 491–501. https://doi.org/10.1007/s00424-001-0735-3.

35. Schmidt-Hieber, C., Jonas, P., and Bischofberger, J. (2007). Subthreshold dendritic signal processing and coincidence detection in dentate gyrus granule cells. J. Neurosci. *27*, 8430–8441. https://doi.org/10.1523/JNEUROSCI.1787-07.2007.

36. Moyer, J.R., and Brown, T.H. (1998). Methods for whole-cell recording from visually preselected neurons of perirhinal cortex in brain slices from young and aging rats. J. Neurosci. Methods *86*, 35–54. https://doi.org/10.1016/s0165-0270(98)00143-5.

37. Aghajanian, G.K., and Rasmussen, K. (1989). Intracellular studies in the facial nucleus illustrating a simple new method for obtaining viable motoneurons in adult rat brain slices. Synapse *3*, 331–338. https://doi.org/10.1002/syn.890030406.

38. Kuenzi, F.M., Fitzjohn, S.M., Morton, R.A., Collingridge, G.L., and Seabrook, G.R. (2000). Reduced long-term potentiation in hippocampal slices prepared using sucrose-based artificial cerebrospinal fluid. J. Neurosci. Methods *100*, 117–122. https://doi.org/10.1016/S0165-0270(00)00239-9.

39. Williams, S.R., and Mitchell, S.J. (2008). Direct measurement of somatic voltage clamp errors in central neurons. Nat. Neurosci. *11*, 790–798. https://doi.org/10.1038/nn.2137.

40. Jonas, P., Major, G., and Sakmann, B. (1993). Quantal components of unitary EPSCs at the mossy fibre synapse on CA3 pyramidal cells of rat hippocampus. J. Physiol. *472*, 615–663. https://doi.org/10.1113/jphysiol.1993.sp019965.

41. Kumar, A., Schiff, O., Barkai, E., Mel, B.W., Poleg-Polsky, A., and Schiller, J. (2018). NMDA spikes mediate amplification of inputs in the rat piriform cortex. eLife *7*, e38446. https://doi.org/10.7554/eLife.38446.

42. Zhu, J.J. (2000). Maturation of layer 5 neocortical pyramidal neurons: amplifying salient layer 1 and layer 4 inputs by Ca2+ action potentials in adult rat tuft dendrites. J. Physiol. *526*, 571.

43. Zhu, J.J. (2023). Architectural organization of ∼1,500-neuron modular minicolumnar disinhibitory circuits in healthy and Alzheimer's cortices. Cell Rep. *42*, 112904. https://doi.org/10.1016/j.celrep.2023.112904.

44. Espinoza, C., Guzman, S.J., Zhang, X., and Jonas, P. (2018). Parvalbumin+ interneurons obey unique connectivity rules and establish a powerful lateral-inhibition microcircuit in dentate gyrus. Nat. Commun. *9*, 4605. https://doi.org/10.1038/s41467-018-06899-3.

45. Shi, Y., and Wang, G. (2024). Protocol to study microcircuits in the medial entorhinal cortex in mice using multiple patch-clamp recordings and morphological reconstruction. STAR Protoc. *5*, 102917. https://doi.org/10.1016/j.xpro.2024.102917.

46. Ruiz, A.J., and Kullmann, D.M. (2012). Ionotropic receptors at hippocampal mossy fibers: roles in axonal excitability, synaptic transmission, and plasticity. Front. Neural Circ. *6*, 112. https://doi.org/10.3389/fncir.2012.00112.

47. Fellenz, M., Schneider, R., Jabra, S., Rietsche, M., Smilovic, D., Vuksic, M., Slattery, D.A., and Deller, T. (2025). Gradual transition of pyramidal cell types in the dorsal hippocampal area CA2b of the C57BL/6 mouse. Sci. Rep. *15*, 29345. https://doi.org/10.1038/s41598-025-04329-1.

48. de No, L. (1934). Studies on the structure of the cerebral cortex. II. Continuation of the study of the ammonic system. Journal für Psychologie und Neurologie 46, 113–177.

49. Xie, A.X., Lauderdale, K., Murphy, T., Myers, T.L., and Fiacco, T.A. (2014). Inducing Plasticity of Astrocytic Receptors by Manipulation of Neuronal Firing Rates. J. Vis. Exp. *85*, 51458. https://doi.org/10.3791/51458.

50. Hamill, O.P., Marty, A., Neher, E., Sakmann, B., and Sigworth, F.J. (1981). Improved patch-clamp techniques for high-resolution current recording from cells and cell-free membrane patches. Pflugers Arch. *391*, 85–100. https://doi.org/10.1007/BF00656997.

51. Engel, D., Pahner, I., Schulze, K., Frahm, C., Jarry, H., Ahnert-Hilger, G., and Draguhn, A. (2001). Plasticity of rat central inhibitory synapses through GABA metabolism. J. Physiol. *535*, 473–482. https://doi.org/10.1111/j.1469-7793.2001.00473.x.

52. Goswami, S.P., Bucurenciu, I., and Jonas, P. (2012). Miniature IPSCs in Hippocampal Granule Cells Are Triggered by Voltage-Gated Ca^{2+} Channels via Microdomain Coupling. J. Neurosci. *32*, 14294–14304. https://doi.org/10.1523/JNEUROSCI.6104-11.2012.

53. Piskorowski, R.A., Nasrallah, K., Diamantopoulou, A., Mukai, J., Hassan, S.I., Siegelbaum, S.A., Gogos, J.A., and Chevaleyre, V. (2016). Age-Dependent Specific Changes in Area CA2 of the Hippocampus and Social Memory Deficit in a Mouse Model of the 22q11.2 Deletion Syndrome. Neuron *89*, 163–176. https://doi.org/10.1016/j.neuron.2015.11.036.

54. Alexander, G.M., Nikolova, V.D., Stöber, T.M., Gruzdev, A., Moy, S.S., and Dudek, S.M. (2025). Perineuronal Nets on CA2 Pyramidal Cells and Parvalbumin-Expressing Cells Differentially Regulate Hippocampal-Dependent Memory. J. Neurosci. *45*, e1626242024. https://doi.org/10.1523/JNEUROSCI.1626-24.2024.

55. San Antonio, A., Liban, K., Ikrar, T., Tsyganovskiy, E., and Xu, X. (2014). Distinct

physiological and developmental properties of hippocampal CA2 subfield revealed by using anti-Purkinje cell protein 4 (PCP4) immunostaining. J. Comp. Neurol. *522*, 1333–1354. https://doi.org/10.1002/cne.23486.

56. Hayani, H., Song, I., and Dityatev, A. (2018). Increased Excitability and Reduced Excitatory Synaptic Input Into Fast-Spiking CA2 Interneurons After Enzymatic Attenuation of Extracellular Matrix. Front. Cell. Neurosci. *12*, 149. https://doi.org/10.3389/fncel.2018.00149.

57. Cope, E.C., Zych, A.D., Katchur, N.J., Waters, R.C., Laham, B.J., Diethorn, E.J., Park, C.Y., Meara, W.R., and Gould, E. (2022). Atypical perineuronal nets in the CA2 region interfere with social memory in a mouse model of social dysfunction. Mol. Psychiatr. *27*, 3520–3531. https://doi.org/10.1038/s41380-021-01174-2.

58. Spruston, N., and Johnston, D. (1992). Perforated patch-clamp analysis of the passive membrane properties of three classes of hippocampal neurons. J. Neurophysiol. *67*, 508–529. https://doi.org/10.1152/jn.1992.67.3.508.

59. Guzman, S.J., Schlögl, A., and Schmidt-Hieber, C. (2014). Stimfit: quantifying electrophysiological data with Python. Front Neuroinf. *8*, 16. https://doi.org/10.3389/fninf.2014.00016.

60. Greger, I.H., and Watson, J.F. (2025). 'Mini analysis' misrepresents changes in synaptic properties due to incomplete event detection. J. Physiol. *603*, 7189–7205. https://doi.org/10.1113/JP288183.

61. Pernía-Andrade, A.J., Goswami, S.P., Stickler, Y., Fröbe, U., Schlögl, A., and Jonas, P. (2012). A Deconvolution-Based Method with High Sensitivity and Temporal Resolution for Detection of Spontaneous Synaptic Currents In Vitro and In Vivo. Biophys. J. *103*, 1429–1439. https://doi.org/10.1016/j.bpj.2012.08.039.

62. Dudek, S.M., Alexander, G.M., and Farris, S. (2023). Introduction to the special issue on: A new view of hippocampal area CA2. Hippocampus *33*, 127–132. https://doi.org/10.1002/hipo.23514.

63. Leroy, F., Brann, D.H., Meira, T., and Siegelbaum, S.A. (2017). Input-Timing-Dependent Plasticity in the Hippocampal CA2 Region and Its Potential Role in Social Memory. Neuron *95*, 1089–1102.e5. https://doi.org/10.1016/j.neuron.2017.07.036.